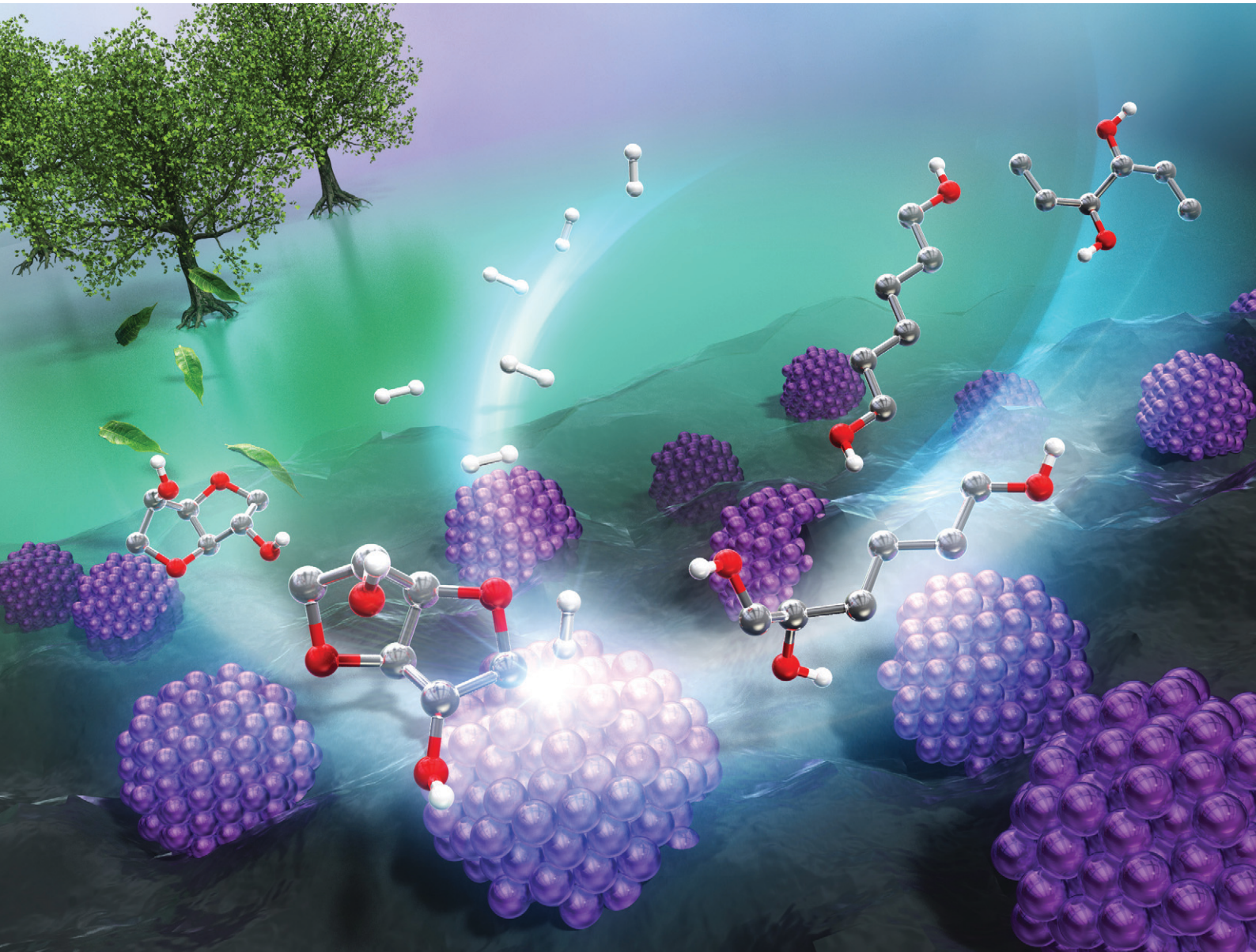


# Catalysis Science & Technology

[rsc.li/catalysis](http://rsc.li/catalysis)



ISSN 2044-4761



Cite this: *Catal. Sci. Technol.*, 2024, 14, 3001

Received 28th February 2024,  
Accepted 8th March 2024

DOI: 10.1039/d4cy00266k

rsc.li/catalysis

Silica-supported Rh (Rh/SiO<sub>2</sub>) was an effective and reusable heterogeneous catalyst for the hydrogenolysis of isosorbide, providing diols and triols in 58% total yield. The yield was higher than those obtained by hydrogenolysis of glucose and sorbitol, confirming the high potential of isosorbide as a biomass-derived intermediate for the synthesis of polyols.

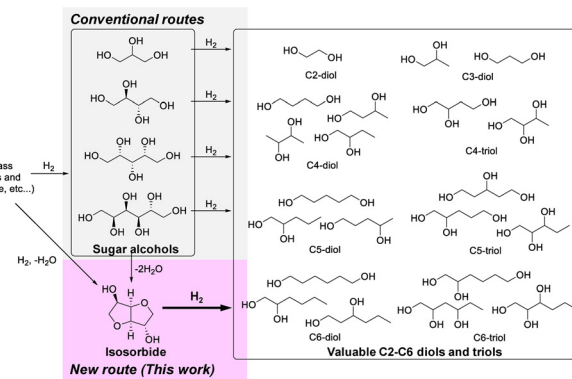
## Introduction

Lignocellulose biomass is the most abundant carbon-based resource on our planet, which has a potential to replace traditional fossil fuels because biomass has renewable and carbon-neutral properties.<sup>1</sup> Development of transformation methods of biomass and biomass-derived intermediates to versatile platform chemicals is critically important to construct a sustainable economy and carbon-neutral society. Among various platform chemicals, diols and triols, carbohydrates with several hydroxyl groups, are fascinating target compounds because they are widely applicable to the synthesis of polymer resins, antifreeze, additives in cosmetics, and transport fuels.<sup>2–5</sup> However, biomass-derived intermediates such as monosaccharides and sugar alcohols, easily available from biomass degradation,<sup>6–10</sup> have high O/C ratios, and therefore, the selective removal of the OH groups is required for the synthesis of the target polyols.

Glucose and xylose, typical monosaccharides, have been applied to the production of C2- or C3-diols such as 1,2-propanediol and ethylene glycol.<sup>11–13</sup> However, these processes are complex and challenging, comprising isomerization, retro-aldol condensation and hydrogenation.<sup>14,15</sup> Extensive focus is on using versatile sugar alcohols such as glycerol, erythritol, xylitol and sorbitol to synthesize polyols *via* selective C–O hydrogenolysis with H<sub>2</sub> as a reducing agent (Scheme 1). For example, the

hydrogenolysis of glycerol can produce 1,2-propanediol *via* the cleavage of terminal OH groups by using noble metal catalysts (Pt, Pd, Rh-based)<sup>16,17</sup> or non-noble metal catalysts (Cu, Ni, Co-based).<sup>18–20</sup> Metal-oxide-modified noble-metal catalysts, such as Pt–WO<sub>x</sub>-based and Ir–ReO<sub>x</sub>-based catalysts, prefer the formation of 1,3-propanediol by the activation of secondary OH groups.<sup>21–23</sup> Erythritol, a C4 molecule produced by the fermentation of glucose,<sup>24</sup> could be converted to butanediols (such as 1,4-, 1,3-, 1,2- and 2,3-butanediol) *via* selective hydrogenolysis over diverse metal-supported catalysts.<sup>25–27</sup> When starting from C5 and C6 sugar alcohols, such as xylitol and sorbitol, which are produced by the hydrogenation of xylose and glucose,<sup>28</sup> C–O dissociation along with C–C hydrogenolysis occurs, producing C2–C6 polyols.<sup>29–32</sup> Moreover, C4–C6 sugar alcohols could be transformed to diols and triols by deoxydehydration in conjunction with hydrogenation over a ReO<sub>x</sub>–Pd/CeO<sub>2</sub> catalyst, where the vicinal OH groups were simultaneously removed.<sup>33,34</sup>

Cyclic sugar derivatives such as alkyl glucosides<sup>35</sup> and anhydrated sugars are also potential starting materials for the synthesis of diols and triols. Deoxydehydration combined



**Scheme 1** The synthesis of valuable diols and triols from typical sugar alcohols and isosorbide (this work) by hydrogenolysis.

Graduate School of Engineering, Osaka Metropolitan University, 3-3-138, Sugimoto, Sumiyoshi-ku, Osaka 558-8585, Japan. E-mail: mtamura@omu.ac.jp  
 † Electronic supplementary information (ESI) available. See DOI: <https://doi.org/10.1039/d4cy00266k>



with hydrogenation of methyl glycosides provides methyl dideoxyglycosides *via* selectively removing *cis*-vicinal OH groups, which were then converted to hexanetriols *via* methoxy bond hydrolysis and hydrogenation.<sup>36–38</sup> Anhydrosugars are useful feedstocks because one OH group in sugar-derived polyols can be selectively reduced by dehydration. 1,4-Anhydroerythritol, a dehydrated C4 product of erythritol, could undergo selective hydrogenolysis to synthesize 1,3- and 1,4-butanediols in various catalyst systems.<sup>39–41</sup> Similarly, C6 anhydrosugars such as isosorbide and sorbitans are potential candidates, however, the transformation has not yet been studied (Scheme 1).

Isosorbide, a stable and commercially available compound derived from glucose, has a peculiar rigid V-shaped structure that incorporates four oxygens in  $\beta$ -position to each other.<sup>42</sup> This unique structure endows isosorbide high thermal stability,<sup>43</sup> decreasing the possibility of the formation of humins. In the transformation of biomass-derived polyols, humin formation from side reactions, which is liable to occur during C6 sugar alcohols hydrogenolysis, is a serious problem because high-temperature reactions are required for the hydrogenolysis of C–O bonds due to the strong bond even with noble metals.<sup>44,45</sup> Moreover, the selective transformation of polyols such as sorbitol and glucose to diols and triols is difficult because polyols have many OH groups with similar reactivities in the flexible alkyl chain. In contrast, isosorbide has two different functional groups, two secondary OH groups and four ether bonds in the rigid structure, and the reactivity difference of these functional groups can be used for the selective transformation. In addition, considering the unique structure of isosorbide, the reactivity of the two OH groups is a little different due to the intramolecular hydrogen bonding, and that of the four ether bonds is also different due to steric hindrance. However, isosorbide is mainly used as the precursor for the formation of solvents and polymers without changing its pristine framework,<sup>46</sup> whereas to our best knowledge, the direct transformation of isosorbide as a starting material to diols and triols has not been reported despite the above potential advantages. Wang *et al.* reported that isosorbide was an important intermediate during sorbitol hydrogenolysis at 523 K over a Pt/NbOPO<sub>4</sub> catalyst, where isosorbide could be transformed to hexane *via* the first ring opening to hexanol and further C–O hydrogenolysis.<sup>47</sup> One of the most favorable target products is  $\alpha,\omega$ -diols such as 1,6-hexanediol and 1,5-pentanediol, which are the most used diols in present chemical industry and are important monomers for the synthesis of polyesters and polycarbonates.<sup>48</sup> Other C6 linear diols such as 1,2-, 1,4- and 1,5-hexanediols and C5 linear diols such as 1,2-, 1,3- and 1,4-pentanediols are also used for polymer syntheses.<sup>49</sup> Therefore, linear diols, particularly,  $\alpha,\omega$ -diols such as 1,6-hexanediol and 1,5-pentanediol, are desirable target diols from isosorbide. Considering the above high potentials of isosorbide, we anticipated the selective transformation of isosorbide would be possible by the development of effective metal-supported catalysts differentiating the functional groups.

Here, we report the synthesis of diols and triols from isosorbide by hydrogenolysis. Silica-supported Rh was found to be an effective and reusable heterogeneous catalyst with high catalytic activity and selectivity to diols and triols.

## Results and discussion

To begin with, the stability of isosorbide was tested at 453 K, since high temperature generally causes the formation of humic products from monosaccharides and sugar alcohols. Negligible conversion (<0.1%) was detected after 4 h in a H<sub>2</sub>SO<sub>4</sub> aqueous solution (pH = 2), suggesting a high thermal stability of isosorbide under reaction conditions.

Next, various SiO<sub>2</sub>-supported noble metal catalysts were applied to isosorbide hydrogenolysis in H<sub>2</sub>O at 453 K for 4 h (Fig. 1). The loading amount of the noble metal was 4 wt%. The formation of isosorbide isomers, tetraols, triols, diols and mono-ols as well as that of alkanes by excessive hydrogenolysis was observed. Triols and diols were mainly composed of cyclic and linear C6 and C5 compounds. In the absence of a catalyst or using SiO<sub>2</sub> as a catalyst, low conversion was observed (<3%). Among the screened metal catalysts, Ru/SiO<sub>2</sub> and Rh/SiO<sub>2</sub> exhibited higher conversion than other catalysts. 68% selectivity to total diols and triols was obtained at 85% conversion over Rh/SiO<sub>2</sub>, while Ru/SiO<sub>2</sub> gave priority to the formation of alkanes (51%) and isomers of isosorbide (34%). The higher activity of Rh/SiO<sub>2</sub> could be ascribed to the superior hydrogenolysis activity of C–OH and C–O–C bonds than those in the case of other noble metals.<sup>50–55</sup> Moreover, it was reported that the ring-opening hydrogenolysis of tetrahydrofurfuryl alcohol (THFA) to 1,2-pentanediol proceeds with comparatively high selectivity (>60%) over the Rh/SiO<sub>2</sub> catalyst,<sup>54</sup> facilitating the ring opening of isosorbide to form cyclic triols. The product formation rate over Rh/SiO<sub>2</sub> (9.69 mmol g<sup>−1</sup> h<sup>−1</sup> at 453 K, 8 MPa H<sub>2</sub> for 4 h) is higher than that reported by Wang *et al.*

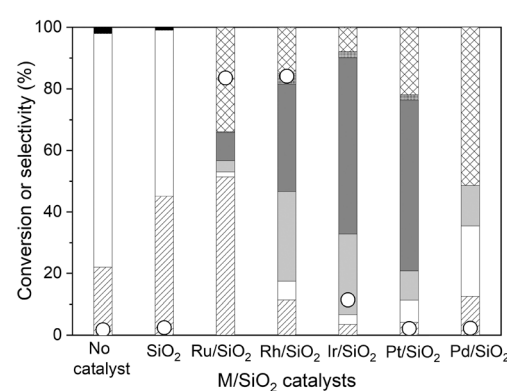


**Fig. 1** Catalytic performances of 4 wt% M/SiO<sub>2</sub> (M = Ru, Rh, Ir, Pt, Pd) catalysts on isosorbide hydrogenolysis. ○: conversion, bars: selectivities (stripe: alkanes, white: mono-ols, gray: diols, dark gray: triols, gray grid: tetraols, across stripe: isomers of isosorbide, black: others). Reaction conditions: 4 g isosorbide, 2 g H<sub>2</sub>O, 0.6 g catalyst, 8 MPa H<sub>2</sub> (at 453 K), 453 K, 4 h.

(3.55 mmol g<sup>-1</sup> h<sup>-1</sup>, Pt/NbOPO<sub>4</sub> at 523 K, 4 MPa H<sub>2</sub> for 4 h)<sup>47</sup> despite of the lower reaction temperature.

The support used for the metal-loaded catalysts plays an important role in the formation of the active sites *via* interaction between metal species and supports, which can affect the catalytic performance. Various Rh/support catalysts were synthesized by using typical metal oxides as supports (SiO<sub>2</sub>, ZrO<sub>2</sub>, Al<sub>2</sub>O<sub>3</sub>, CeO<sub>2</sub>, MgO), and the performance was compared (Fig. 2). Rh/SiO<sub>2</sub> showed the highest conversion with diols and triols as main products, followed by Rh/ZrO<sub>2</sub>. Low conversion of isosorbide was observed when using Rh/γ-Al<sub>2</sub>O<sub>3</sub>, Rh/CeO<sub>2</sub> and Rh/MgO with more generation of isosorbide isomers. Generally, OH groups can be adsorbed on basic sites strongly<sup>56,57</sup> probably to suppress the access to the active Rh metal sites or destabilize the transition state, leading to the low conversion. Moreover, the reducibility of the Rh metal is also important, and inert supports such as SiO<sub>2</sub> and C are suitable for the complete reduction of Rh species.<sup>53</sup> Therefore, inert SiO<sub>2</sub> which has almost no basicity and acidity is a suitable support for the reaction.

The Rh/SiO<sub>2</sub> catalysts were characterized by H<sub>2</sub>-TPR, XRD and TEM analyses. Fig. 3(A) shows the TPR profile of Rh/SiO<sub>2</sub>. The signal due to the reduction of Rh species was observed below the reaction temperature of 453 K with a Rh reduction degree >99%, indicating that Rh species in Rh/SiO<sub>2</sub> was in the metallic state.

Fig. 3(B) shows the XRD patterns of Rh/SiO<sub>2</sub> catalysts. The catalyst after calcination (b) showed a broad signal around 34°, which was assigned to RhO<sub>x</sub> species. After the reaction ((c)–(h)), signals at 41°, 47° and 70° due to the Rh metal and no signals due to RhO<sub>x</sub> were observed, indicating Rh species were reduced to the metallic state. These results are in agreement with the abovementioned H<sub>2</sub>-TPR results. The particle size of the Rh metal was calculated to be 3.9 nm from XRD, which was further confirmed by TEM analysis (Fig. 3(C) and (D)), where the aggregation of Rh particles did not occur.

Next, the effect of reaction parameters such as H<sub>2</sub> pressure, reaction temperature and isosorbide concentration

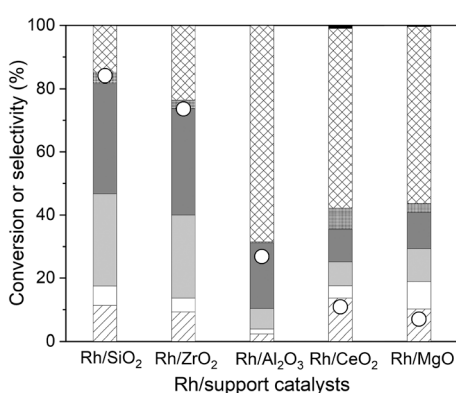


Fig. 2 Catalytic performances of Rh/support (Rh = 4 wt%, support = SiO<sub>2</sub>, ZrO<sub>2</sub>, Al<sub>2</sub>O<sub>3</sub>, CeO<sub>2</sub>, MgO) catalysts on isosorbide hydrogenolysis. O: conversion, bars: selectivities (stripe: alkanes, white: mono-ols, gray: diols, dark gray: triols, gray grid: tetraols, across stripe: isomers of isosorbide, black: others). Reaction conditions: 4 g isosorbide, 2 g H<sub>2</sub>O, 0.6 g catalyst, 8 MPa H<sub>2</sub> (at 453 K, 453 K, 4 h).

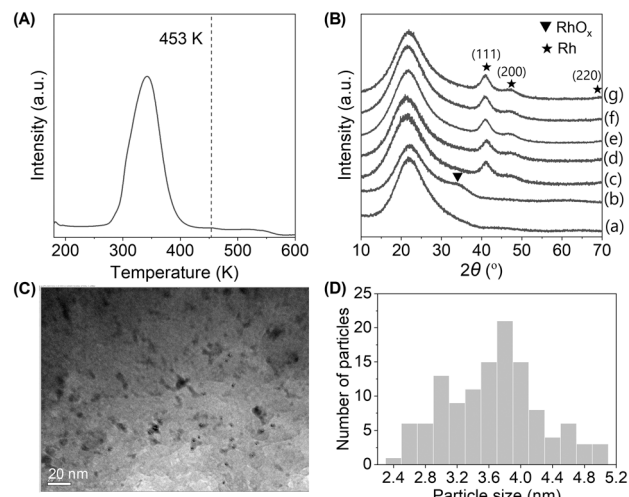


Fig. 3 Characterization of Rh/SiO<sub>2</sub>. (A) TPR profile of Rh/SiO<sub>2</sub>, (B) XRD patterns of Rh/SiO<sub>2</sub>, (a) SiO<sub>2</sub>, (b) RhO<sub>x</sub>/SiO<sub>2</sub> after calcination, (c) Rh/SiO<sub>2</sub> at 0 h reaction, (d) Rh/SiO<sub>2</sub> at 1 h reaction, (e) Rh/SiO<sub>2</sub> at 4 h reaction, (f) Rh/SiO<sub>2</sub> at 6 h reaction, and (g) Rh/SiO<sub>2</sub> at 8 h reaction. (C) TEM image of used Rh/SiO<sub>2</sub> catalyst after 4 h reaction. (D) Rh particle distribution.

was investigated over Rh/SiO<sub>2</sub>. The H<sub>2</sub> pressure was in the range of 2–8 MPa (Fig. S1 and Table S1†). At a low H<sub>2</sub> pressure of 2 MPa, only 37% of isosorbide was converted even after 12 h reaction. The conversion linearly increased with increasing the H<sub>2</sub> pressure, and at 8 MPa H<sub>2</sub> it reached 96% after 8 h. The selectivity to diols and triols increased with increasing H<sub>2</sub> by comparing them at the same conversion level (Table S1,† selectivity: 48% (2 MPa) to 69% (8 MPa)), indicating that H<sub>2</sub> pressure exhibited a positive effect on the activity and selectivity towards diols and triols over Rh/SiO<sub>2</sub>. This phenomenon is consistent with previous reports where the activation of H<sub>2</sub> is an important step in the hydrogenolysis process.<sup>21,23</sup>

The reaction temperature also exhibited a positive effect on the conversion of isosorbide in the range of 433 K to 473 K (Table S2†). The maintained high carbon balance (94% after 4 h) even at 473 K implied the good stability of isosorbide during the reaction. Besides, the selectivity to diols and triols was rarely influenced by temperatures. Considering the conversion and yield, the reaction at 453 K was selected for the following study.

The isosorbide concentration dependence on the hydrogenolysis over Rh/SiO<sub>2</sub> was investigated (Fig. S2 and Table S3†). The conversion dramatically increased with the increase in the concentration from 3 to 7 M along with the increased selectivity to diols and triols. At higher concentrations ranging from 7 to 27 M, the conversion and selectivity were almost the same, suggesting that the adsorption of isosorbide was saturated over Rh/SiO<sub>2</sub>. Considering that the concentration in the standard reaction conditions was set at 14 M, isosorbide is adequately supplied to the catalyst surface under the standard reaction conditions.

We further compared the hydrogenolysis activity of other C6 sugars such as isomannide, sorbitol and glucose with that of isosorbide at similar conversion levels (Fig. S3†). The hydrogenolysis of isomannide also selectively formed diols and triols but with a much lower conversion rate of  $0.8 \text{ mmol h}^{-1}$  compared to that of isosorbide ( $19 \text{ mmol h}^{-1}$ ). The low reactivity was also observed when using sorbitol ( $0.8 \text{ mmol h}^{-1}$ ) and glucose ( $0.9 \text{ mmol h}^{-1}$ ) as starting materials, where tetraols by random removal of OH groups in the structure, as well as small alkanes by the C–C cleavage, were obtained as main products, while the selectivity to diols and triols was low. Moreover, carbon balance obviously decreased in the cases of sorbitol (91%) and glucose (72%), which would be due to the poor thermal stability under reaction conditions and the formation of humins. These results confirmed that isosorbide is a promising substrate for the synthesis of diols and triols with higher reaction activity.

The reusability of  $\text{Rh/SiO}_2$  was evaluated in the hydrogenolysis of isosorbide (Table S4†). There were no significant differences in the conversion and product yields between fresh and spent  $\text{Rh/SiO}_2$  catalysts. The particle size of Rh species was maintained around  $3.7\text{--}3.9 \text{ nm}$  (Fig. S4†), suggesting good stability of  $\text{Rh/SiO}_2$ .

The time course of isosorbide hydrogenolysis over  $\text{Rh/SiO}_2$  at 453 K and 8 MPa  $\text{H}_2$  is shown in Fig. 4 (Table S5†). The reaction

smoothly proceeded to reach 96% conversion at 8 h. At the initial stage of 26% conversion at 0 h, the isomers of isosorbide were mainly produced in 10% yield (selectivity: 41%), which gradually decreased at longer reaction times. The yield of triols first increased from 0 to 1 h and then leveled off (around 27–29%) when prolonging the reaction time. A monotonously increased tendency was observed in diol yield with respect to reaction time. The maximum total yield of diols and triols was obtained at 8 h reaction with 58% (29% for each), and their distributions are shown in Fig. 4(b) and (c). A mixture of cyclic and linear C6 compounds was observed in triols, which can be formed by the partial and complete tetrahydrofuran ring open, respectively. Determination of the structure of C6 triols is difficult due to the similar mass patterns. 1,6-Hexanediol (5%) and 3,4-hexanediol (7%) were identified as the main C6 linear diols, although cyclic and linear C6 diols were also formed.

From the time trend of products (Fig. 4), isosorbide is transformed into triols by hydrogenolysis and then further hydrogenolysis of the triols occurs to provide diols (probably some compounds are produced *via* the formation of tetraols). Based on previous reports on the hydrogenolysis of polyols and ethers over  $\text{Rh/SiO}_2$ ,<sup>50–53,58,59</sup> the possible formation route of the identified main products of 1,6-hexanediol and 3,4-hexanediol is proposed (Scheme 2): the first step will be mainly the hydrogenolysis of either one of the C–O bonds in the ether bond (C–O–C) of isosorbide to provide triols with one tetrahydrofuran ring (cyclic C6 triols),<sup>50,51,58</sup> and then further hydrogenolysis of the ether bond (C–O–C) of the tetrahydrofuran ring in the cyclic C6 triols provides the corresponding tetraols (1,2,5,6-hexanetetraol and 2,3,4,5-hexentetraol). 1,2,5,6-Hexanetetraol will be mainly converted to 1,6-hexanediol because the selectivity of the C–O bond dissociation of the secondary OH group is quite high (~87%) in the hydrogenolysis of propylene glycol over  $\text{Rh/SiO}_2$ .<sup>52</sup> 2,3,4,5-Hexentetraol can be converted to 3,4-hexanediol. Considering the higher reactivity of the linear vicinal OH groups than that of the ether bond in the cyclic ethers,<sup>53</sup> the small formation amount of tetraols can be explained by the reactivity of linear vicinal OH groups. Moreover, the formation of C2–C5 diols was also observed, suggesting that degradation of C6 products such as C–C bond hydrogenolysis occurred in some contents, which is in good accordance with the previous report on hydrogenolysis of polyols over Rh catalysts.<sup>53,59</sup> A more detailed reaction route is under investigation.

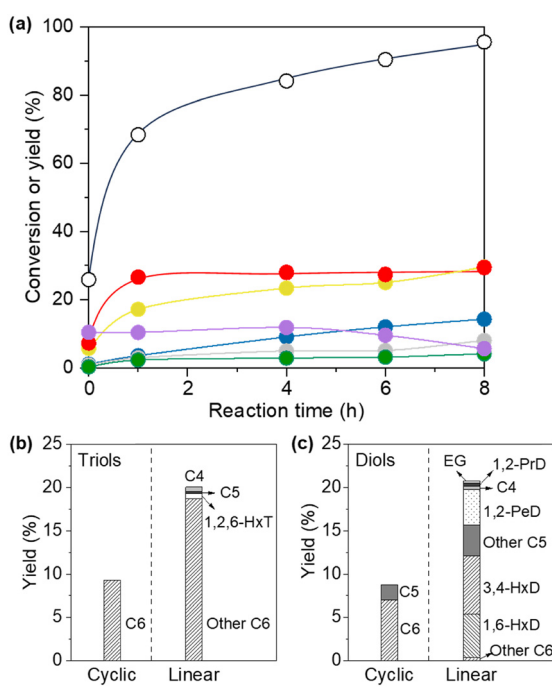
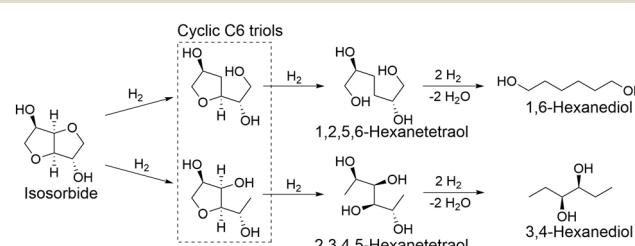


Fig. 4 (a) The time course of hydrogenolysis of isosorbide over  $\text{Rh/SiO}_2$  under optimized conditions. ○: conversion, colored circles: selectivities (blue: alkanes, gray: mono-ols, yellow: diols, red: triols, green: tetraols, purple: isomers of isosorbide). (b) Triol distribution at 8 h reaction, 1,2,6-HxT = 1,2,6-hexanetriol. (c) Diol distribution at 8 h reaction, 1,6-HxD = 1,6-hexanediol, 3,4-HxD = 3,4-hexanediol, 1,2-PeD = 1,2-pentanediol, 1,2-PrD = 1,2-propandiol, EG = ethylene glycol. Reaction conditions: 4 g isosorbide, 2 g  $\text{H}_2\text{O}$ , 0.6 g  $\text{Rh/SiO}_2$  ( $\text{Rh} = 4 \text{ wt\%}$ ), 8 MPa  $\text{H}_2$  (at 453 K), 453 K.



Scheme 2 Plausible formation routes of main C6 diols (1,6-hexanediol and 3,4-hexanediol) from isosorbide by hydrogenolysis over  $\text{Rh/SiO}_2$ .



## Conclusion

We found that isosorbide is a promising compound for the synthesis of valuable diols and triols due to its high stability. Rh/SiO<sub>2</sub> acted as an effective and reusable heterogeneous catalyst for the hydrogenolysis of isosorbide, providing 58% total yield of target products. The characterization of the catalysts by XRD, TPR and TEM analyses suggested that metallic Rh species with 3.9 nm metal particles on the catalyst work as active sites. Moreover, Rh/SiO<sub>2</sub> showed good reusability and stability after four cycles without significant change in the particle size of Rh species.

## Author contributions

Pengru Chen: investigation, formal analysis, and writing – original draft. Wataru Onodera: investigation and formal analysis. Masato Akatsuka: formal analysis. Yusuke Kita: formal analysis. Masazumi Tamura: conceptualization, funding acquisition, formal analysis, supervision, and writing – review & editing.

## Conflicts of interest

There are no conflicts to declare.

## Acknowledgements

This study was supported by the Environment Research and Technology Development Fund [JPMEERF21S11910].

## Notes and references

- 1 P. Sudarsanam, R. Zhong, S. V. Bosch, S. M. Coman, V. I. Parvulescu and B. F. Sels, *Chem. Soc. Rev.*, 2018, **47**, 8349.
- 2 A. Corma, S. Iborra and A. Velty, *Chem. Rev.*, 2007, **107**, 2411.
- 3 Y. Wang, F. Wang, Q. Song, Q. Xin, S. Xu and J. Xu, *J. Am. Chem. Soc.*, 2013, **135**, 1506.
- 4 D. B. Klinedinst, I. Yilgör, E. Yilgör, M. Zhang and G. L. Wilkes, *Polymer*, 2012, **53**, 5358.
- 5 Y. Gu, M. Tamura, Y. Nakagawa, K. Nakao, K. Suzuki and K. Tomishige, *Green Chem.*, 2021, **23**, 5786.
- 6 H. Kobayashi, Y. Ito, T. Komanoya, Y. Hosaka, P. L. Dhepe, K. Kasai, K. Hara and A. Fukuoka, *Green Chem.*, 2011, **13**, 326.
- 7 A. Shrotri, H. Kobayashi and A. Fukuoka, *Acc. Chem. Res.*, 2018, **51**, 761.
- 8 P. Chung, A. Charmot, O. A. Olatunji-Ojo, K. A. Durkin and A. Katz, *ACS Catal.*, 2014, **4**, 302.
- 9 P. Chen, A. Shrotri and A. Fukuoka, *ChemSusChem*, 2019, **12**, 2576.
- 10 P. H. Galebach, D. J. McClelland, N. M. Eagan, A. M. Wittrig, J. S. Buchanan, J. A. Dumesic and G. W. Huber, *ACS Sustainable Chem. Eng.*, 2018, **6**, 4330.
- 11 Y. Liu, Y. Liu and Y. Zhang, *Appl. Catal., B*, 2019, **242**, 100.
- 12 M. Gu, Z. Shen, W. Zhang, M. Xia, J. Jiang, W. Dong, X. Zhou and Y. Zhang, *ChemCatChem*, 2020, **12**, 3447.
- 13 A. Aho, S. Engblom, K. Eränen, V. Russo, P. Mäki-Arvela, N. Kumar, J. Wärnå, T. Salmi and D. Y. Murzin, *Chem. Eng. J.*, 2021, **405**, 126945.
- 14 M. Zheng, J. Pang, R. Sun, A. Wang and T. Zhang, *ACS Catal.*, 2017, **7**, 1939.
- 15 M. Lv, Y. Zhang, Q. Xin, D. Yin, S. Yu, S. Liu, L. Li, C. Xie, Q. Wu, H. Yu and Y. Liu, *Chem. Eng. J.*, 2020, **396**, 125274.
- 16 Y. Nakagawa and K. Tomishige, *Catal. Sci. Technol.*, 2011, **1**, 179.
- 17 Q. Sun, S. Wang and H. Liu, *ACS Catal.*, 2017, **7**, 4265.
- 18 S. Wang, Y. Zhang and H. Liu, *Chem. – Asian J.*, 2010, **5**, 1100.
- 19 X. Guo, Y. Li, R. Shi, Q. Liu, E. Zhan and W. Shen, *Appl. Catal., A*, 2009, **371**, 108.
- 20 E. Ryneveld, A. S. Mahomed, P. S. Heerden, M. J. Green and H. B. Friedrich, *Green Chem.*, 2011, **13**, 1819.
- 21 Y. Amada, Y. Shinmi, S. Koso, T. Kubota, Y. Nakagawa and K. Tomishige, *Appl. Catal., B*, 2011, **105**, 117.
- 22 J. Wang, X. Zhao, N. Lei, L. Li, L. Zhang, S. Xu, S. Miao, X. Pan, A. Wang and T. Zhang, *ChemSusChem*, 2016, **9**, 784.
- 23 L. Liu, S. Kawakami, Y. Nakagawa, M. Tamura and K. Tomishige, *Appl. Catal., B*, 2019, **256**, 117775.
- 24 Y. Nakagawa, T. Kasumi, J. Ogihara, M. Tamura, T. Arai and K. Tomishige, *ACS Omega*, 2020, **5**, 2520.
- 25 M. Gu, L. Liu, Y. Nakagawa, C. Li, M. Tamura, Z. Shen, X. Zhou, Y. Zhang and K. Tomishige, *ChemSusChem*, 2021, **14**, 642.
- 26 L. Liu, J. Cao, Y. Nakagawa, M. Betchaku, M. Tamura, M. Yabushita and K. Tomishige, *Green Chem.*, 2021, **23**, 5665.
- 27 W. Wang, K. Nakagawa, T. Yoshikawa, T. Masuda, E. Fumoto, Y. Koyama, T. Tago and H. Fujitsuka, *Appl. Catal., A*, 2021, **619**, 118152.
- 28 H. Kobayashi, Y. Hosaka, K. Hara, B. Feng, Y. Hirosaki and A. Fukuoka, *Green Chem.*, 2014, **16**, 637.
- 29 Q. Xia, G. Zhang, J. Wang, W. Zhang, M. Liu, Y. Li, B. Yin, C. Yang, J. Shen and X. Jin, *Ind. Eng. Chem. Res.*, 2020, **59**, 13879.
- 30 H. Liu, Z. Huang, H. Kang, X. Li, C. Xia, J. Chen and H. Liu, *Appl. Catal., B*, 2018, **220**, 251.
- 31 X. Jin, J. Shen, W. Yan, M. Zhao, P. S. Thapa, B. Subramaniam and R. V. Chaudhari, *ACS Catal.*, 2015, **5**, 6545.
- 32 Y. Yu, Q. Zhang, X. Chen, Y. Liu, Y. Qin, S. Qiu, H. Li and T. Wang, *Fuel Process. Technol.*, 2020, **197**, 106195.
- 33 N. Ota, M. Tamura, Y. Nakagawa, K. Okumura and K. Tomishige, *Angew. Chem., Int. Ed.*, 2015, **54**, 1897.
- 34 N. Ota, M. Tamura, Y. Nakagawa, K. Okumura and K. Tomishige, *ACS Catal.*, 2016, **6**, 3213.
- 35 A. Karam, K. D. O. Vigier, S. Marinkovic, B. Estrine, C. Oldani and F. Jérôme, *ACS Catal.*, 2017, **7**, 2990.
- 36 S. H. Krishna, J. Cao, M. Tamura, Y. Nakagawa, M. D. Bruyn, G. S. Jacobson, B. M. Weckhuysen, J. A. Dumesic, K. Tomishige and G. W. Huber, *ACS Sustainable Chem. Eng.*, 2020, **8**, 800.
- 37 M. Tamura, N. Yuasa, J. Cao, Y. Nakagawa and K. Tomishige, *Angew. Chem., Int. Ed.*, 2018, **57**, 8058.



38 J. Cao, M. Tamura, R. Hosaka, A. Nakayama, J. Hasegawa, Y. Nakagawa and K. Tomishige, *ACS Catal.*, 2020, **10**, 12040.

39 T. Wang, M. Tamura, Y. Nakagawa and K. Tomishige, *ChemSusChem*, 2019, **12**, 3615.

40 L. Liu, T. Asano, Y. Nakagawa, M. Tamura and K. Tomishige, *Green Chem.*, 2020, **22**, 2375.

41 K. Tomishige, M. Yabushita, J. Cao and Y. Nakagawa, *Green Chem.*, 2022, **24**, 5652.

42 F. Aricò, A. S. Aldoshin and P. Tundo, *ChemSusChem*, 2017, **10**, 53.

43 J. Hong, D. Radojčić, M. Ionescu, Z. S. Petrović and E. Eastwood, *Polym. Chem.*, 2014, **5**, 5360.

44 S. Luo, J. Li, J. Ran, R. Yangcheng, Y. Cui, Y. Zhang and J. Wang, *Catal. Commun.*, 2023, **175**, 106614.

45 A. Aho, S. Engblom, K. Eränen, V. Russo, P. Mäki-Arvela, N. Kumar, J. Wärnåa, T. Salmi and D. Murzin, *J. Chem. Eng.*, 2021, **405**, 126945.

46 W. Qian, X. Tan, Q. Su, W. Cheng, F. Xu, L. Dong and S. Zhang, *ChemSusChem*, 2019, **12**, 1169.

47 J. Xi, Q. Xia, Y. Shao, D. Ding, P. Yang, X. Liu, G. Lu and Y. Wang, *Appl. Catal., B*, 2016, **181**, 699.

48 Y. Gu, M. Tamura, Y. Nakagawa, K. Nakao, K. Suzukic and K. Tomishige, *Green Chem.*, 2021, **23**, 5786.

49 B. M. Stadler, A. Brandt, A. Kux, H. Beck and J. G. Vries, *ChemSusChem*, 2020, **13**, 556.

50 S. Koso, N. Ueda, Y. Shinmi, K. Okumura, T. Kizuka and K. Tomishige, *J. Catal.*, 2009, **267**, 89.

51 S. Koso, Y. Nakagawa and K. Tomishige, *J. Catal.*, 2011, **280**, 221.

52 A. Shimao, S. Koso, N. Ueda, Y. Shinmi, I. Furikado and K. Tomishige, *Chem. Lett.*, 2009, **38**, 540.

53 I. Furikado, T. Miyazawa, S. Koso, A. Shimao, K. Kunimori and K. Tomishige, *Green Chem.*, 2007, **9**, 582.

54 Y. Nakagawa and K. Tomishige, *Catal. Today*, 2012, **195**, 136.

55 K. Chen, K. Mori, H. Watanabe, Y. Nakagawa and K. Tomishige, *J. Catal.*, 2012, **294**, 171.

56 M. Tamura and K. Tomishige, *Angew. Chem., Int. Ed.*, 2015, **54**, 864.

57 D. R. Mullins, S. D. Senanayake and T. L. Chen, *J. Phys. Chem. C*, 2010, **114**, 17112.

58 T. Arai, M. Tamura, Y. Nakagawa and K. Tomishige, *ChemSusChem*, 2016, **9**, 1680.

59 Y. Shinmi, S. Koso, T. Kubota, Y. Nakagawa and K. Tomishige, *Appl. Catal., B*, 2010, **94**, 318.

